Reinforced Concrete Columns Insulated by Different Gypsum Layers Exposed to 900°C One Side Fire Flame

Mohanad Salih Farhan Al-Jadiri
Department of Civil Engineering, University of Baghdad, Iraq
m.farhan1901p@coeng.uobaghdad.edu.iq (corresponding author)

Abdul Muttalib I. Said
Department of Civil Engineering, University of Baghdad, Iraq
Dr.AbdulMuttalib.I.Said@coeng.uobaghdad.edu.iq

Received: 2 June 2023 | Revised: 3 July 2023 and 5 July 2023 | Accepted: 16 July 2023

 DOI: https://doi.org/10.48084/etasr.6083

ABSTRACT

This study investigated the effect of high-temperature fire flame on reinforced concrete columns coated with a layer of gypsum insulation. Six samples were cast and cured in a hot water bath at 67°C, covered on one side by 10 and 20 mm thick layers of gypsum plaster. The samples were exposed to a 900°C fire flame in a hydrocarbon fire furnace for one and two hours. The results showed that the gypsum plaster layer prevented a high-temperature rise within the core of the column. The differences between all gypsum-coated columns varied compared to those of the reference samples. The gypsum-coated columns had reduced axial displacements and no spalling and visible cracks on their faces. The improvement in the compressive strength of concrete will be discussed in a future paper. This study was carried out following ACI-318 and ASTM C1529.

Keywords-hydrocarbon fire; one face; temperature evolution; ASTM 1529

I. INTRODUCTION

Experimental research on gypsum plasterboards involves setting them ablaze with simulated fire. In [1], a large-scale fire test was conducted on steel stud gypsum plasterboards to evaluate their fire resistance. The results showed that mechanical stress had little impact on the thermal behavior of gypsum plasterboards. An increase in cracks was induced by applying both temperature and load whereas the features of the material that were temperature-dependent could be detected. The thermal properties of the materials change as a result of the heating and cooling processes. In [2], a multi-phase approach was followed to predict heat transfer within the gypsum layer under fire exposure, including conduction, mass transfer, and condensation/evaporation, and considering water vapor transport and condensation in the porous structure. The calculated temperatures above 100°C were adequate up to 2 cm from the fireside and a numerical model was proposed to calculate the temperatures in the gypsum blocks for longer distances. Experimental investigations of gypsum plasterboards were performed under exposure to natural fire, and thermal properties were determined for both the heating and cooling phases. The results of a large-scale fire test on loaded steel beams were extracted, and the fire protection behavior was tested under a standard fire curve, both with and without mechanical load.

In [3], the thermal behavior of gypsum plasterboards for steel elements was investigated by exposure to natural fire. The results showed a clear dependence on the heating and cooling rate, while the thermal material properties changed within the heating and cooling phase. In [4], a simple two-dimensional model was validated to predict heat transfer through gypsum-board/wood-stud walls exposed to fire. In [5], the influence of depth and distance between studs on the fire resistance of Lightweight Timber-Framed (LTF) walls lined with gypsum plasterboards was investigated, using numerical simulations and experimental tests. In [6], the fire protection performance of gypsum board assemblies was investigated, presenting a hybrid numerical-experimental method to extract the thermal conductivity of various gypsum products at elevated temperatures, performing high-temperature mechanical tests and developing a 2D finite element model to simulate the structural performance of gypsum boards in a fire. In [7], the high-temperature exposure of normal concrete covered with gypsum plaster layers was studied. The experimental results showed that concrete with gypsum layers at 400 and 700°C had less losses in compressive strength, modulus of rupture, and modulus of elasticity. In [8], the results of exposure to 400 and 700°C of normal concrete covered with gypsum and plaster layers were presented, showing that their ultimate load capacity and load-deflection curves were better than the uncoated reference samples.

This study investigated the effect of high-temperature fire flame on reinforced concrete columns coated with 10 and 20 mm thick gypsum insulation layers. Six samples were cast and cured in a hot water bath at 67°C, covered on one side by 10 and 20 mm thick layers of gypsum plaster, and then exposed to a 900°C fire flame in a hydrocarbon fire furnace. Three samples, without coating (R), with a 10 mm gypsum coating (1G), and with a 20 mm gypsum coating (2G), were exposed to fire for 1 hr, and 3 respective samples were exposed for 2 hr.

II. THE EXPERIMENT

The tests on the square reinforced concrete columns were conducted at the site of Reyah Al-Moasem, a concrete provider company. The experimental procedure consisted of 6 fire tests supporting both ends of the column. Two columns were used as reference samples without having a protective cover, two columns were covered with 10mm gypsum, and the last two columns were covered with 20mm gypsum. All columns were subjected to the same fire and time conditions, at 900° C for one or two hours. The tests simulated an actual fire scenario in a building to observe the effect of a gypsum layer on the reinforced concrete column by one face of fire exposure.

III. TEST SET-UP

A. Characteristics of the Specimens

The test specimens were reinforced concrete columns having 1500 mm height and 150×150 mm cross-sections. Concrete had a compressive strength of 28 MPa and the steel reinforcement bar had a yield of 418 MPa. After 24 hr of accelerated curing at 67°C, the specimens were ready to test. All specimens were similar in dimensions, steel reinforcement, curing time, concrete compressive strength, and number of stirrups. Gypsum layers of 10 and 20 mm thickness were attached to the respective specimens. A 1750×1250×750 mm water tank was used, connected to a thermometer and having three 3000 W electric heaters. The water was heated to 67°C with a curing duration of approximately 24 hr to reach maximum strength [9]. All specimens were prepared with reinforcement bars and stirrups of 12 and 6 mm diameter and assembled as a frame according to ACI-318 [10]. To strengthen the column, a 50×50×3 mm square steel plate was fixed at both ends, rounding the ends. Preparation of the specimen started with connecting the main reinforcement bars and stirrups. The reinforcement bars were then carefully placed inside the mold to achieve the desired concrete cover. All specimens were instrumented with Type-K thermocouples, placed in three sections along their vertical direction, each containing 5-6 thermocouples, as shown in Figure 1. Then, the steel hooks and longitudinal reinforcement bars were connected to the stirrups by wires. After these steel works and the concrete casting, the specimens were left to cure in the hot water tank.

B. Mechanical Properties

Coarse aggregate sized 4-19, C28 compressive concrete, and reinforcing steel bars of 418 MPa yield were used for all test specimens. The concrete cover related to the stirrups for all tested columns was 20 mm on each side.

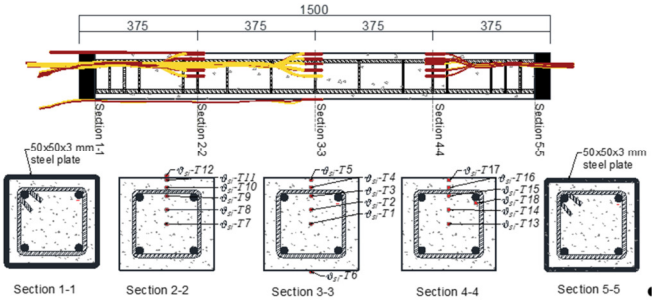

Fig. 1. Thermocouple's location through column sample cross-section.

C. Specimens Preparation

The specimens were placed in the furnace horizontally. The longitudinal steel reinforcement bars were traditionally framed according to ACI-318 [10]. The main steel reinforcement area bars were selected to have the same ratio values per cross-section for all specimens tested. All specimens were cast identically and all the column specimens were exposed to furnace fire flame. The inside dimensions of the furnace were 500×650×1250 mm, it could be opened from both ends, and the heating was provided by propane gas designed to cover all the perimeter exposed to direct fire flame. Figure 2 shows the design of the furnace. Each top and bottom side contained 10 gas jets. The furnace sides had 5 jets each. Each jet group for all sides was connected to the master gas hose in a separate way to make it more easily used and controlled by a gas valve regulator. The furnace was covered by 200×100×50 mm thermal insulation bricks and had holes to allow the flame to pass through the propane gas tube to the interior of the furnace perimeter.

D. Test Installation

Figures 2 and 3 show a broad view of the experimental devices. The furnace was constructed using cast steel and insulating blocks to maintain the required temperature for the duration of the test. According to ACI-318 [10], the specimen was placed horizontally inside the furnace. The fire was directed at the upper face and right side to give the entire column specimen the highest amount of exposure to fire. The sections were 375, 750, and 1125 mm from the base of the column, respectively, and the thermocouples were positioned within the column specimen at three levels in the cross-section. The furnace was capable of reaching temperatures of 1300°C and applying fire curves with various heating rates. This study used the ASTM 1529 standard fire curve [11].

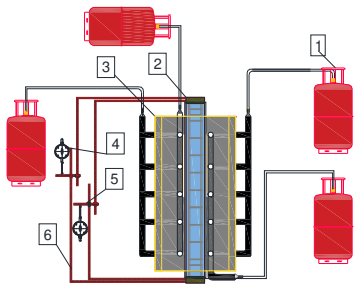

Fig. 2. Top view of the furnace system.

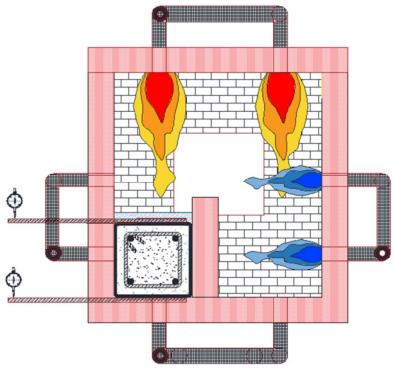

Fig. 3. Front view for furnace system cross-section.

Type-K thermocouples, installed at 5 different levels through the cross-sections of the tested columns, were used to measure the temperatures of the specimens. Six thermocouples were evenly distributed throughout each cross-section, one attached to the longitudinal and transverse reinforcement bars and the others embedded in the concrete at varying depths: the first one close to the surface, the second near the center, the third in the middle between them, and the fourth one close to the stirrups at the top level. Four shielded type-K thermocouples were used to monitor the temperatures within the furnace during the tests. A 24-channel temperature-capable data logger was used to collect the data. The two ends of the column specimens were connected by two steel bars that were welded to them, and the other two sides were fastened with a steel plate with holes cut for one steel bar to allow the other to move freely [12-14]. The second dial gauge was positioned using the same process on the bottom side. One thermocouple was positioned between the gypsum layer and the column's face to record the temperature passage to the column's concrete face. All dial gauges were placed outside the furnace for maximum heat protection.

E. Test Method

This study aimed to investigate how the gypsum layer influences a structural member's capacity to survive fire by exposing concrete column specimens to flames that imitate actual fire accident conditions. This test aimed to achieve 900°C and document the differences in temperature between all specimens, describing temperature-related deformation. Thermal elongation occurred while the test specimens were exposed to the fire and were manually captured by a camera with a time stamp for the test application. The temperature was recorded between the four insulated thermocouples placed on four sides of the specimens. The specimens were exposed for one and two hours at temperatures of 900°C, with the gypsum coating on one face of the column being 10mm and 20mm thick, respectively. The specimens were heated to their maximum fire exposure and brought to the desired temperature in 8 to 12 minutes [11].

Fig. 4. Test installation and samples.

IV. RESULTS AND ANALYSIS

A. Temperature Evolution

Concrete elements are affected to different degrees by the heat generated by fire for a certain period. Figures 5-8 show that the temperature begins to rise linearly for all specimens covered with a gypsum layer, while the temperature rise is steady and non-linear in uncoated specimens. Table I shows the temperature values recorded by the thermocouples T1, T2, T3, T4, and T5 and their variation over time. The temperature increases by more than twice in the core of the uncoated specimens through the surface area. This increase is slower for specimens covered with a gypsum protection layer during the burning period of 1 hr. Increasing the fire exposure period leads to higher temperatures. For the uncoated reference specimens, this increase reached its peak in the area near the surface (T5), unlike the specimens protected by the gypsum layer, where the temperature rise was gradual and almost constant and did not exceed 313°C when exposed to a flame temperature exceeding 900°C for a burning period of two continuous hours.

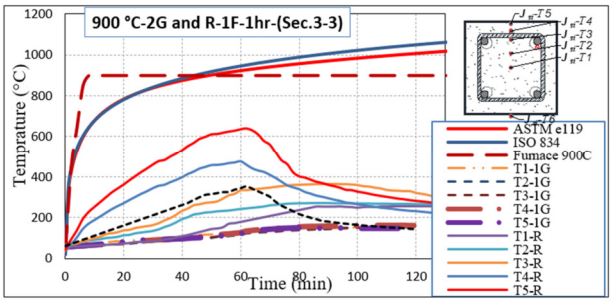

Fig. 5. Time-temperature comparison for R and 2G in cross-sections.

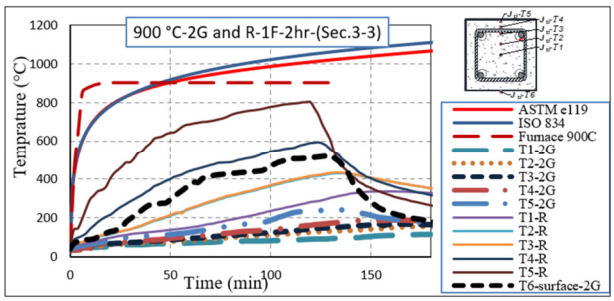

Fig. 7. Time-temperature comparison for R and 2G in cross-sections.

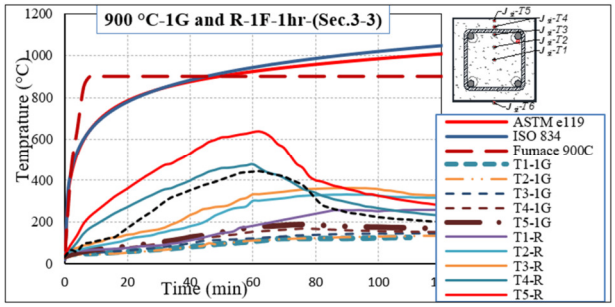

Fig. 6. Time-temperature comparison for R and 1G in cross-sections.

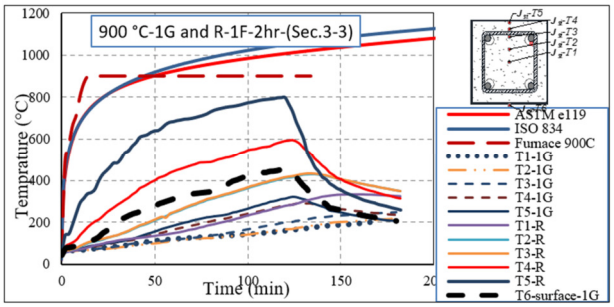

Fig. 8. Time-temperature comparison for R and 1G in cross-sections.

TABLE I. TEMPERATURE VALUES THROUGH THERMOCOUPLES

Column reference	Gypsum layer thickness (mm)	Fire exposure duration (min)	Range of exposure (min)	T1 (ºC)	T2 (ºC)	T3 (ºC)	T4 (ºC)	T5 (ºC)	T-surface (ºC)	T-rebar (ºC)
Sq-R-900-1F-1h-L	0	60	R30	88.5	106.5	157.5	178.5	231	900	146
			R60	186	190.5	325.5	439.5	642	900	231
Sq-1G-900-1F-1h-L	10	60	R30	58	65	75	96	101	275	65
			R60	95	111	119	154	176	442	112
Sq-2G-900-1F-1h-L	20	60	R30	75	82	83	89	93	210	83
			R60	115	115	117	126	132	342	109
Sq-R-900-1F-2h-L	0	120	R30	114	139	140	284	505	900	150
			R60	149	246	249	443	685	900	238
			R90	209	336	340	512	756	900	315
			R120	280	413	417	591	800	900	382
Sq-1G-900-1F-2h-L	10	120	R30	74	78	84	105	107	202	65
			R60	110	111	116	164.5	184	311	112
			R90	130	131	149	222	240	386	155
			R120	149	166	198	281	313	451	218
Sq-2G-900-1F-2h-L	20	120	R30	55	69	74	78	100	141	83
			R60	67	87	96	104	125	271	119
			R90	77	107	118	132	170	327	146
			R120	84	127	143	161	235	373	176

TABLE II. TEMPERATURE REDUCTION RATIO

Column reference	Range of Exposure (min)	Reduction ratio %						
		T1 %	T2 %	T3 %	T4 %	T5 %	T-surface %	T-rebar %
Sq-1G-900-1F-1h-L	R30	34.46	38.96	52.38	46.21	56.27	69.44	55.47
	R60	48.92	41.73	63.44	64.96	72.58	53.11	51.51
Sq-2G-900-1F-1h-L	R30	15.25	23.0	47.3	50.14	59.74	76.55	43.15
	R60	38.17	39.63	64.0	71.33	79.43	62.00	52.81
Sq-1G-900-1F-2h-L	R30	35	43.88	40.0	57.66	78.81	77.55	65.66
	R60	26.17	54.87	53.41	62.86	73.13	65.44	52.94
	R90	37.79	61.0	56.17	56.64	68.25	57.11	50.79
	R120	46.78	59.8	52.51	52.45	60.87	49.88	42.93
Sq-2G-900-1F-2h-L	R30	51.75	50.35	47.14	68.54	80.19	84.33	38.0
	R60	55.0	64.63	61.44	76.52	81.75	69.88	50.0
	R90	63.15	68.15	65.29	74.21	77.51	63.66	53.65
	R120	70.0	69.24	65.7	72.75	70.62	58.55	53.92

B. Thermal Reduction Comparison

The reference columns (R) experienced high-temperature values compared with the specimens covered by 10 (1G) and 20 mm (2G) gypsum plaster cover, noted as 1G and 2G, respectively. Table II shows the temperature reduction ratios for all thermocouple recordings. The differences between Sq-R-900-1F-1h-L and Sq-1G-900-1F-1h-L show that the reduction in temperature values was about 34.46%, 38.96%, 52.38%, 46.21%, and 56.27% for thermocouples T1, T2, T3, T4, and T5, respectively, for 30 min of fire exposure. For the same specimens and thermocouples, the reduction ratios were 48.92%, 41.73%, 63.44%, 64.96%, and 72.58% after 60 min of fire exposure. For the specimens Sq-R-900-1F-1h-L and Sq-2G-900-1F-1h-L, the temperature reduction was 15.25%, 23%, 47.3%, 50.14%, and 59.74% for 30 min of exposure and 38.17%, 39.63%, 64%, 71.33%, and 79.43%, respectively, for 60 min. The comparison between specimens Sq-R-900-1F-2h-L and Sq-1G-900-1F-2h-L showed temperature reductions of 35%, 43.88%, and 40.0%, 57.66%, and 78.81%, for 30 min, 26.17%, 54.87%, 53.41%, 62.86%, and 73.13%, and 37.79%, for 60 min, 61.0%, 56.17%, 56.64%, and 68.25%, and 46.78%, for 90 min, and 59.8%, 52.51%, 52.45%, and 60.87% for 120 min of exposure. The specimens Sq-R-900-1F-2h-L and Sq-2G-900-1F-2h-L showed respective reductions of 51.7%, 50.35%, 47.1%, 68.54%, and 80.19% for 30 min, 55.0%, 64.63%, 61.44%, 76.52%, and 81.75% for 60 min, 63.15%, 68.15%, 65.29%, 74.21%, and 77.51% for 90 min, and 70.0%, 69.24%, 65.7%, 72.75%, and 70.62% for 120 min of exposure.

A thermocouple was placed between the gypsum plaster cover and the face of the concrete to study the direct fire exposure reduction between the reference and the covered specimens. The gypsum plaster cover indicated a large compartment of heat transfer between the specimens. The difference in temperature for Sq-R-900-1F-1h-L and Sq-1G-900-1F-1h-L was 69.44% and 53.11% for 30 and 60 min of fire exposure, respectively. For Sq-R-900-1F-1h-L and Sq-2G-900-1F-1h-L the difference was 76.55% and 62.00% for 30 and 60 min, respectively. The temperature reduction ratios between Sq-R-900-1F-2h-L and Sq-2G-900-1F-2h-L were 84.33%, 69.88%, 63.66%, and 58.55%, for 30, 60, 90, and 120 min of fire exposure. These results show that the temperature reduction varied for all covered column specimens, indicating that the most useful gypsum protection layer was in Sq-2G-900-1F-2h-L, which showed maximum protection.

The temperature in the cross-section center (T1) throughout the gypsum layer was reduced by 58.55% to the rest of the column fibers, showing that they resisted the fire effect on both concrete and rebars efficiently. For 60 min of fire exposure, the temperature reduction values were convergent and efficient in protecting the specimen. The gypsum protection layer efficiently affected the rebar temperature conductivity, as the temperature was lower by 55.47% and 51.51% for 30 and 60 min exposure for Sq-1G-900-1F-1h-L. The temperature of Sq-2G-900-1F-1h-L was lower by 43.15% and 52.81% for 30 and 60 min of fire. For Sq-1G-900-1F-2h-L and Sq-2G-900-1F-2h-L, the temperature reductions was 65.66%, 52.94%, 50.79 and 42.93, and 38.0%, 50.0%, 53.65% and 53.92%, for 30, 60, 90, and 120 min of fire exposure, respectively.

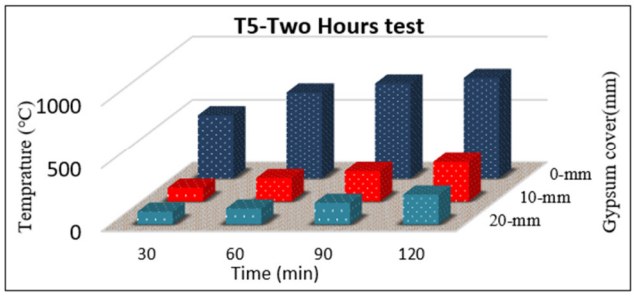

Fig. 9. Temperature values comparison in T5 with time.

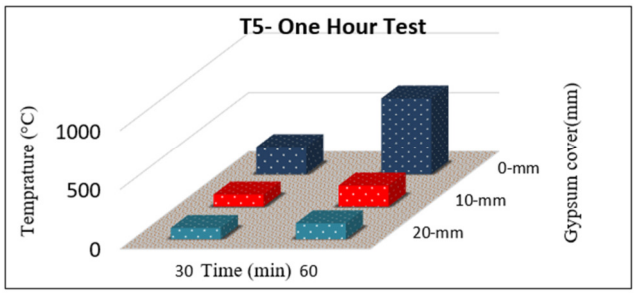

Fig. 10. Temperature values comparison in T5 with time.

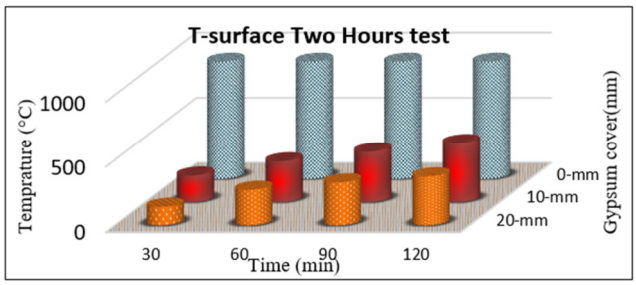

Fig. 11. Temperature comparison for 120 min duration.

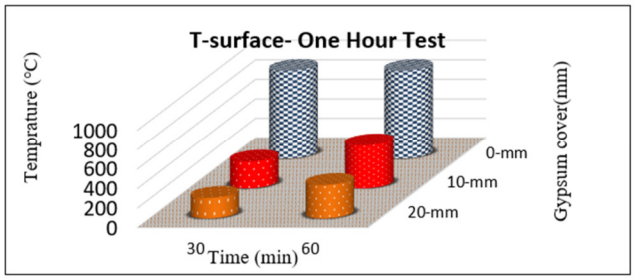

Fig. 12. Temperature comparison for 60 min duration.

The thermal behavior and performance of the gypsum were significantly influenced by its moisture content, as it dissociates and evaporates at elevated temperatures [7]. Therefore, the thermal properties of gypsum are temperature-dependent. Gypsum shrinkage at high temperatures is the main cause of the structural failure of gypsum layers in a fire. Gypsum shrinks at varying rates depending on the thickness of the layer due to the non-uniform temperature that causes thermal strains along it. As gypsum loses strength at high temperatures, the mechanical stresses caused by the restrained thermal strains eventually cause cracks. Fire resistance of

gypsum board assemblies is considerably affected by gypsum fall-off in the fire. As a result, gypsum manufacturers are constantly looking for ways to make their gypsum board products more structurally effective. It is sensible to investigate whether gypsum products with reduced shrinkage rates perform better structurally in fire-related situations [6].

C. Axial Displacements

The axial displacements measured by the dial gauges can trace their evolution in time. Figure 13 shows a comparison of the obtained axial displacements. The axial displacements increased to a maximum and then decreased under the axis of the initial position. Initially, due to high temperatures, the column elongates and then shrinks with the degradation of the mechanical properties of concrete and reinforcing steel. The axis of the initial position is not crossed at the same time as the restraining forces because their relationship with the column's axial displacement is non-linear. The axial displacement values vary due to the high temperature, indicated as positive and negative values. The maximum axial displacements of the coated specimens were approximately 3.85 and 5.3 mm, respectively, for the side exposed directly to the fire flame, as shown in Table IV and Figure 13(a)-(b). In the coated specimens, the axial displacements were taken by two dial gauges on the top (exposed to direct fire flame) and bottom (non-exposed) sides. Figure 13 (c)-(f) shows that the maximum axial displacements were 2.5, 4.687, 0.91, and 0.43 mm, for the specimens exposed to direct fire flame and 1.46, 3.58, 2.67, and 1.195 mm for indirect heating flow.

TABLE III. RESULTS AFTER THE TIME OF FIRE EXPOSURE FOR ALL COLUMNS TEST

Column reference	Gypsum layer thickness (mm)	Time of exposure to fire (min)	T5 max (°C)	(T-surface) max (°C)	$((T_R - T_G)/T_R)$ %	$((T_{surf.}-TG)/T_{surf.})$ %	Θ_{rebar} max (°C)	Rebar-Heat reduction %	ΔLmax (mm)		Spalling observation
									Top	Bottom	
Sq-R-900-1F-1h-L	0	60	642	900	0	0	342	0	3.85	*	yes
Sq-R-900-1F-2h-L	0	120	800	900	0	0	382	0	5.3	*	yes
Sq-1G-900-1F-1h-L	10	60	176	422	72.52	53.11	112	67.25	2.5	1.46	No
Sq-1G-900-1F-2h-L	10	120	313	451	60.87	49.88	219	42.67	4.687	3.58	No
Sq-2G-900-1F-1h-L	20	60	132	342	79.43	62.00	109	68.12	0.91	2.67	No
Sq-2G-900-1F-2h-L	20	120	235	373	70.62	58.55	176	53.92	0.43	1.195	No

(*) not recorded

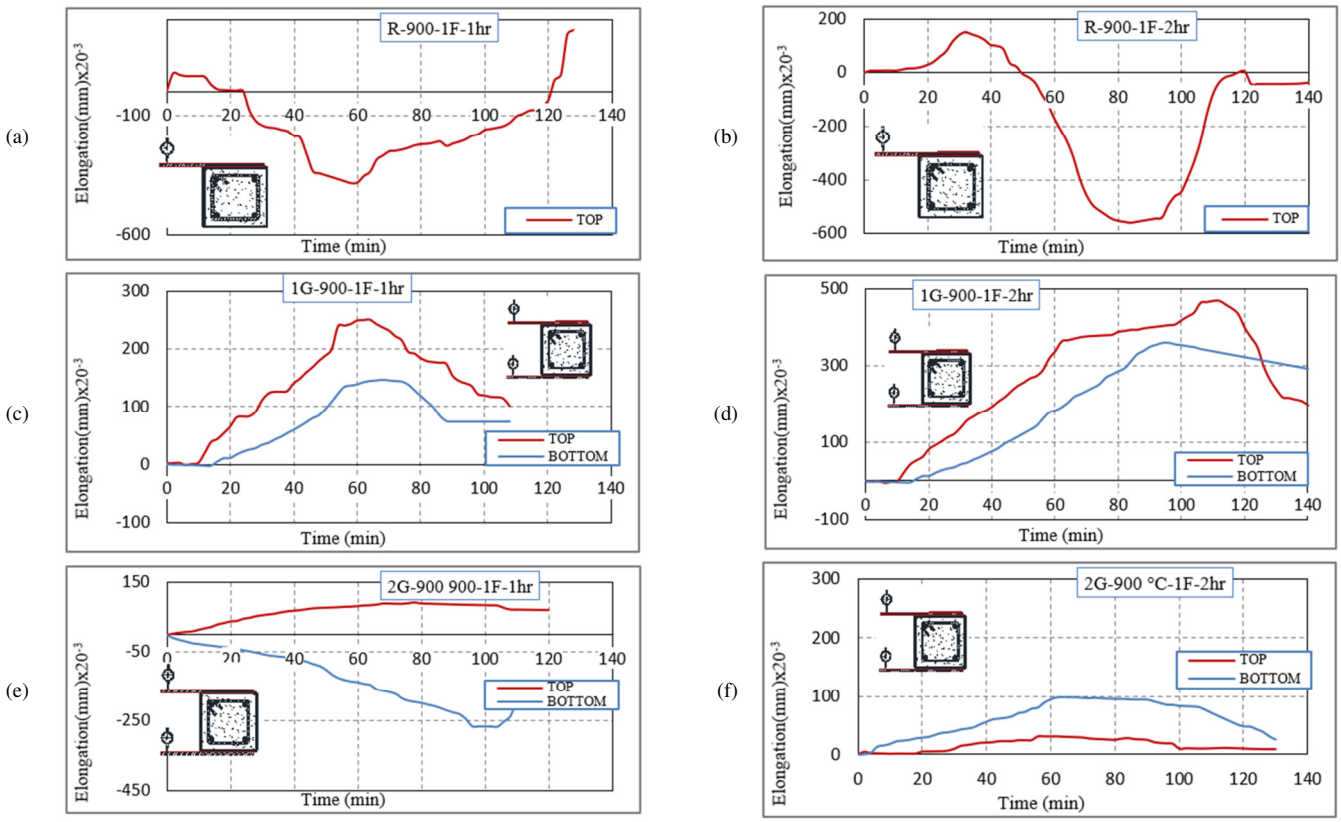

Fig. 13. Time-axial displacement due to high temperature.

V. CONCLUSION AND DISCUSSION

Unprotected reinforced concrete parts exposed to extreme heat behave differently from the coated ones. The results of this study showed that the use of a gypsum plaster layer to protect reinforced concrete columns exposed to direct fire flame reduced one third the amount of heat penetrated during the period of higher exposure compared to unprotected ones. The gaps in the plaster material dissipate the heat reaching the body of the column and, therefore, the residual heat penetrates the section-cross of the column down to the core area, as well as the presence of moisture content in the plaster can reduce the effect of heat for a certain period.

CREDIT AUTHOR STATEMENT

Abdul Muttalib I.Said: Conceptualization, methodology, writing, review, and editing. Mohanad Salih Farhan: Writing the original draft preparation and carrying out the experimental tests.

REFERENCES

[1] D. Norsk, A. Sauca, and K. Livkiss, "Fire resistance evaluation of gypsum plasterboard walls using machine learning method," *Fire Safety Journal*, vol. 130, Jun. 2022, Art. no. 103597, https://doi.org/10.1016/j.firesaf.2022.103597.

[2] R. Prieler *et al.*, "Modelling approach to predict the fire-related heat transfer in porous gypsum based on multi-phase simulations including water vapour transport, phase change and radiative heat transfer," *Applied Thermal Engineering*, vol. 206, Apr. 2022, Art. no. 118013, https://doi.org/10.1016/j.applthermaleng.2021.118013.

[3] J. Zehfuß and L. Sander, "Gypsum plasterboards under natural fire—Experimental investigations of thermal properties," *Civil Engineering Design*, vol. 3, no. 3, pp. 62–72, 2021, https://doi.org/10.1002/cend.202100002.

[4] J. R. Mehaffey, P. Cuerrier, and G. Carisse, "A model for predicting heat transfer through gypsum-board/wood-stud walls exposed to fire," *Fire and Materials*, vol. 18, no. 5, pp. 297–305, 1994, https://doi.org/10.1002/fam.810180505.

[5] P. A. G. Piloto, S. Rodríguez-del-Río, and D. Vergara, "Fire Analysis of Timber-Framed Walls Lined with Gypsum," *Materials*, vol. 15, no. 3, Jan. 2022, Art. no. 741, https://doi.org/10.3390/ma15030741.

[6] I. Rahmanian, "Thermal and mechanical properties of gypsum boards and their influences on fire resistance of gypsum board based systems," Ph.D. dissertation, University of Manchester, Manchester, UK, 2011.

[7] R. S. Warwar and A. I. Said, "Mechanical Properties of Normal Strength Concrete Covered with Gypsum Layers and Exposed to High Temperatures (Fire Flame)," in *Geotechnical Engineering and Sustainable Construction*, Singapore, 2022, pp. 641–656, https://doi.org/10.1007/978-981-16-6277-5_51.

[8] R. S. Warwar and A. I. Said, "Flexural Behavior of Reinforced Concrete Beams Covered by Gypsum Layers and Exposed to Elevated Temperatures," in *E3S Web of Conferences - Second International Conference on Geotechnical Engineering*, Iraq, 2021, vol. 318, Art. no. 03005, https://doi.org/10.1051/e3sconf/202131803005.

[9] "Standard Test Method for Static Modulus of Elasticity and Poisson's Ratio of Concrete in Compression," American Society for Testing and Materials, West Conshohocken, PA, USA, Standard ASTM C469-02, 2002.

[10] ACI Comittee 318, "Building Code Requirements for Structural Concrete (ACI 318-19) - Commentary (ACI 318R-19)," American Concrete Institute, Farmington Hills, MI, USA, ACI 318R-19, 2019. https://doi.org/10.14359/51716937.

[11] "Standard Test Methods for Determining Effects of Large Hydrocarbon Pool Fires on Structural Members and Assemblies" American Society for Testing and Materials, West Conshohocken, PA, USA, Standard ASTM E1529-22.

[12] A. M. Al-Hilali, A. F. Izzet, and N. Oukaili, "Static Shear Strength of a Non-Prismatic Beam with Transverse Openings," *Engineering, Technology & Applied Science Research*, vol. 12, no. 2, pp. 8349–8353, Apr. 2022, https://doi.org/10.48084/etasr.4789.

[13] A. J. Daraj and A. H. Al-Zuhairi, "The Combined Strengthening Effect of CFRP Wrapping and NSM CFRP Laminates on the Flexural Behavior of Post-Tensioning Concrete Girders Subjected to Partially Strand Damage," *Engineering, Technology & Applied Science Research*, vol. 12, no. 4, pp. 8856–8863, Aug. 2022, https://doi.org/10.48084/etasr.5008.

[14] H. Q. Abbas and A. H. Al-Zuhairi, "Flexural Strengthening of Prestressed Girders with Partially Damaged Strands Using Enhancement of Carbon Fiber Laminates by End Sheet Anchorages," *Engineering, Technology & Applied Science Research*, vol. 12, no. 4, pp. 8884–8890, Aug. 2022, https://doi.org/10.48084/etasr.5007.